Journal of Modern Optics, 2015
Vol. 62, No. 19, 1583–1590, http://dx.doi.org/10.1080/09500340.2015.1052582

Singly resonant sum-frequency generation of 520-nm laser via a variable input-coupling transmission cavity

Shanlong Guo, Yulong Ge, Jun He and Junmin Wang*

State Key Laboratory of Quantum Optics and Quantum Optics Devices, and Institute of Opto-Electronics, Shanxi University, Tai Yuan, P.R. China

(*Received 21 December 2014; accepted 13 May 2015*)

We experimentally present a three-mirror folded singly resonant sum-frequency generation (SFG) cavity with an adjustable input coupling, which has been applied to 520-nm single-frequency laser generation via 780-nm laser and 1560-nm laser frequency mixing in a periodically poled $KTiOPO_4$ crystal (PPKTP). A continuous variation in the input coupling reflectivity from 81.4 to 96.1% for 780-nm resonant laser is achieved by tilting the input coupler, and the impedance matching of the resonator can be optimized. Up to 268 mW of SFG output power at 520-nm is obtained with 6.8 W of the 1560-nm laser input and 1.5 W of 780-nm laser input.

Keywords: sum-frequency generation (SFG); 520-nm single-frequency laser; erbium-doped fiber amplifier (EDFA); singly resonant cavity; variable transmissivity input coupler; PPKTP bulk crystal

1. Introduction

Coherent light sources in the green spectral region play an important role in scientific and technical research, such as atomic physics, medical applications, laser printing and display. 520-nm green laser in this spectral region is of special interest. It can be used to excite Cs atoms from the $6P_{3/2}$ state to the 39D Rydberg states to create ultracold Rydberg plasma [1]. Frequency doubling of 520-nm laser can produce 260-nm laser, which is often needed for (non-resonant) photo-detachment of atoms or molecules [2]. Additionally, in the field of quantum information, 520-nm continuous-wave (CW) laser can be used as pump laser to generate two-color entangled optical fields of 1560 and 780-nm by optical parametric oscillator (OPO) or optical parametric amplifier (OPA) [3,4], which can be potentially implemented in quantum repeater protocol via entanglement swapping [5]. To get a better performance in above cases, the 520-nm laser source is expected for higher output power, better beam quality, and lower noise.

Many methods can be used to get 520-nm laser sources. Laser emitted directly by single-frequency diode lasers is a simple way, but the output power is limited, and beam quality is not desirable. It can be an attractive solution to take the χ^2 process to achieve a high conversion efficiency, for example, the second-harmonic generation (SHG) and also the sum-frequency generation (SFG). Early in 2004, Brunner et al. presented an average power of 23 W at 515-nm laser in a single-pass frequency doubling configuration of a 5 mm-long lithium triborate (LBO) crystal by a mode-locked thin disk Yb:YAG laser [6]. In 2011, Rothhardt et al. demonstrated a high-average-power femtosecond laser system at 520-nm with 135 W average power at a pulse repetition rate of 5.25 MHz, and the beam quality factor was $M^2 < 1.2$ [7]. In a CW laser region, Jensen et al. took a high power distributed Bragg reflector (DBR) tapered diode laser at 1062-nm, more than 1.5 W of green light at 531-nm was generated by single-pass SHG in a periodically poled MgO-doped lithium niobate (MgO:PPLN), a conversion efficiency of 18.5% was achieved in the experiments [8]. Laser, they reported a tapered diode laser operated in a coupled ring cavity to efficiently generate more than 500 mW green laser output power at 530 to 533-nm with a $LiNbO_3$ crystal, and the optical–optical conversion efficiency exceeded 30% [9]. In order to make a further increase in output power, the cascaded nonlinear crystals system has also been implemented in the experiments. In 2014, Hansen et al. described the generation of 3.5 W of diffraction-limited green light from SHG of a single 10 W tapered diode laser at 1063-nm with two cascaded MgO:PPLN crystals [10]. Additionally, the laser–seeded fiber amplifier has been used as the fundamental wave source to the frequency doubling. In 2008, Pullen et al. reported a 2.3 W green laser frequency doubling from the fiber laser amplifier at 1029-nm in a single-pass configuration of MgO:PPLN crystal [11]. Also, in 2010, Tu et al. demonstrated an ultrashort, compact green light radiation by frequency doubling of an all-fiber ytterbium-doped fiber laser source in a periodically poled

*Corresponding author. Email: wwjjmm@sxu.edu.cn

$KTiOPO_4$ (PPKTP) waveguide, and over 300 mW of picosecond radiation at 532-nm was obtained for a fundamental power of 1.6 W, corresponding to a conversion efficiency of 19.3% [12]. Similarly, SFG which combined two fundamental waves mixing in a nonlinear crystal also shows a good performance in generation of green laser. Mi [13] employed intra-cavity SFG of two infrared beams around 1030 and 1048-nm to get 260 mW of 520-nm laser in a type-I critical phase-matching LBO crystal; Vasilyev et al. [14] also reported a single-pass configuration of periodically poled stoichiometric lithium tantalate (PPSLT) crystal, which have achieved a power of 1.2 W at 522-nm laser by single-passs SFG of 1565- and 782.5-nm lasers. Improvement of the fundamental power is another way to achieve a high harmonic wave generation. By combining the two DBR tapered diode lasers, Müller et al. showed a maximum output power of 3.9 W green light generating in a MgO:PPLN by SFG at a total input power of 15.7 W, and the corresponding optical–optical conversion efficiency is 24.8% [15]. Moutzouris et al. reported a highly efficient third harmonic generation of 55 mW at 520-nm using fan-out poled MgO:PPLN crystal, and an overall conversion efficiency of 9.2% was obtained [16]. PPKTP crystal offers lager effective nonlinear coefficient (d_{eff} ~10 pm/V), wider temperature acceptance bandwidth and lower photorefractive damage threshold, and it is also an attractive quasi-phase-matched (QPM) material candidate for CW green generation. However, the related SFG work of 520-nm laser generation based on PPKTP crystal has been little reported now. In our experiment, we take PPKTP as SFG crystal, combining 1560 and 780-nm laser as pump lasers to get 520-nm laser with a singly resonant enhancement configuration.

This approach offers many advantages. As we known, the laser at 520-nm is just the third harmonic wave of 1560-nm. Benefiting from the large market of optical fiber lasers, the telecom C-band 1560-nm fiber components developed maturely and are stable in property. They can provide CW high fundamental wave output power and also make the master oscillator power amplifier (MOPA) laser systems based on the fiber amplifier commercially available [17,18]. Meanwhile, frequency-doubled 1560-nm is corresponding to the rubidium D_2 transition line; thus, an optical frequency standard can be realized by locking to the atomic absorption line, attaining a stable frequency characteristic of the entire laser system [19]. Furthermore, using of an enhanced cavity configuration, we can make a higher conversion efficiency for SHG output, and this scheme also saves the phase matching adjustment of cascaded crystals in the single-pass configuration [14,20]. The resonant enhancement cavity technology is also effective in SFG. No matter doubly resonant-external cavity SFG system or the singly resonant external-cavity SFG system have both shown superior SFG output power performance [21,22]. Compared with the doubly resonant SFG system, more stable system characteristic exhibited for the singly resonant system [23]. Moreover, a singly resonate system can be more widely adopted in the SFG experiments whose enhancement cavity cannot be locked resonantly with the two fundamental waves simultaneously [14]. Such a 520-nm SFG laser system applied to the OPA can directly offer the local oscillators of the down-conversion optical fields at 1560 and 780 nm, which is used as homodyne detector to measure the entanglement characteristic of the generated two-color optical fields [4,24].

The key of the resonant enhancement technology is to increase the intra-cavity circulating power of the fundamental waves. To address this, the passive loss of the enhancement system to the fundamental should be first reduced as much as possible. On this basis, when the input coupling of the resonator equals to the sum of its passive loss and nonlinear conversion depletion (impedance matching), there can be a higher intra-cavity circulating power in the resonator.

The main difficulty is that the actual passive loss of the enhancement system is very low, which cannot be easily measured directly, meanwhile the nonlinear conversion depletion is also variable with different input fundamental power levels, so the accurate input coupling cannot be readily determined. The traditional technique in search of input coupling relies on the replacement of different input coupler mirrors with discrete transmission values at the resonant wavelength. This approach requires different input coupler mirrors to obtain the optimum value of input coupling. However, different mirrors will lead to new rounds of different passive losses of the resonator, which makes absolute optimization of impendence matching of the resonator inefficient and costly.

Here, we demonstrated an alternative new approach for absolute optimized improved three-mirror standing-wave SFG cavity instead of conventional two-mirror standing-wave cavity or the four-mirror traveling-wave cavity. As simple *in situ* tilting of the input coupler varies the incident angle of the resonant fundamental wave, the three-mirror cavity exploits the ability to adjust the input coupling; at the same time, the tilting will not change the waist spot size and position of the fundamental waves in the crystal.

In this study, a relatively simple and practical SFG scheme to 520-nm CW green radiation has been presented. Based on the singly resonant SFG in PPKTP crystal by mixing 1560- and 780-nm lasers, output power of 268 mW at 520-nm laser is obtained. The experimental results are basically consistent with our theoretical calculations.

2. Theoretical analysis of singly resonant sum-frequency generation

For ensuring a higher output power of the singly resonant SFG configuration, the key requirement is to make both fundamental waves intra-cavity circulating power greater. To the non-resonant laser, we can just increase the incident power; but to the resonant laser, it still needs to finetune to the reflectivity of input coupler. Appropriate reflectivity of the input coupler can lead to a higher intra-cavity circulating power, and hence the higher nonlinear conversion; the inappropriate reflectivity cannot make maximum level of lasers coupled to the cavity, but reflected from the cavity. Additionally, to the SFG, it also should consider the nonlinear depletions of two fundamental waves, for they are nonlinear coupled with each other.

It can be a recommended approach to consider all the factors above by plotting of the sum-frequency output power as a function of input coupling. For a given set of input laser sources, cavity components, and the nonlinear coupling coefficient, the SFG output power can be generally described as [25]:

$$P_3 = \gamma_{\mathrm{SFM}} P_{\mathrm{c},1} P_{\mathrm{c},2}, \tag{1}$$

where γ_{SFM} shows the single-pass SFG conversion efficiency of the crystal for the two fundamental waves, and $P_{\mathrm{c},i}(i = 1, 2)$ represents the circulating powers in the resonator at 1560- and 780-nm lasers.

And the $P_{\mathrm{c},1}$, $P_{\mathrm{c},2}$ are written:

$$P_{\mathrm{c},1} = P_{\mathrm{i},1}\left[1 - \left(\delta_1 + \frac{\omega_1}{\omega_1 + \omega_2}\gamma_{\mathrm{SFM}} P_{\mathrm{c},2}\right)\right], \tag{2}$$

$$P_{\mathrm{c},2} = P_{\mathrm{i},2}\frac{1 - R_{\mathrm{i},2}}{\left\{1 - \left\{R_{\mathrm{i},2}\left[1 - \left(\delta_2 + \frac{\omega_2}{\omega_1+\omega_2}\gamma_{\mathrm{SFM}} P_{\mathrm{c},1}\right)\right]\right\}^{1/2}\right\}^2}, \tag{3}$$

where δ_1 and, δ_2 are nonlinear conversion depletion for two fundamental waves at 1560 and 780-nm, and $P_{\mathrm{i},1}$ and $P_{\mathrm{i},2}$ are the incident power at 1560 and 780-nm, respectively. ω_1 and ω_2 are the frequency at 1560 and 780-nm, the $R_{\mathrm{i},2}$ is the reflectivity of input coupler at 780-nm. The detailed derivation process of the above Equation (2) and (3) can be found in the Appendix 1. If all parameters in Equation (2) and (3) are known, they can be taken into Equation (1), thus the plots can be done.

Figure 1 shows contour plots of the 520-nm output as a function of the reflectivity of the input coupler at 780 and 1560-nm input with a fixed input powers at 780-nm (1.5 W), fixed nonlinear coupling coefficient (1.2%/W), and fixed resonator passive losses of 3% at 780-nm and 2% at 1560-nm.

From the theoretical simulations, we can find the singly resonant 520-nm output power is determined both by 1560-nm incident power and the reflectivity of 780-nm input coupler under definite cavity parameters. A combination of ~6.8 W of 1560-nm laser and ~1.5 W of 780-nm laser can provide maximum ~0.4 W of 520-nm output. There exists an optimum reflectivity at 780-nm (impedance matching) to make the SFG output power maximum for each fixed 1560-nm incident power. And the region of reflectivity which is higher than optimum (under-coupled), the SFG output power decreases much

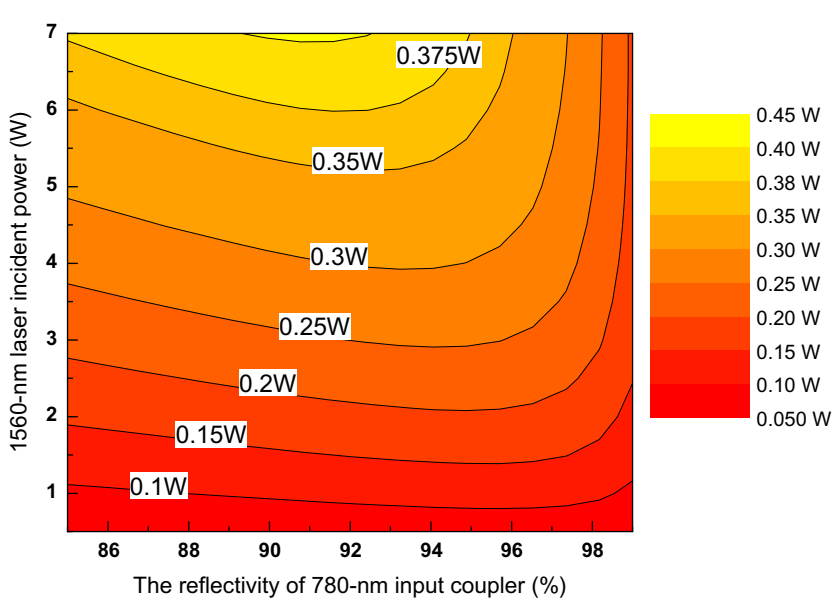

Figure 1. Contour plot of the predicted output power at 520-nm as a function of the reflectivity of the input coupler mirror at 780-nm and incident power at 1560-nm. (The color version of this figure is included in the online version of the journal.)

faster than the region of reflectivity which is lower than the optimum (over-coupled).

3. Experimental setup and results

The experimental scheme is shown schematically in Figure 2. The seed light source we used is an external-cavity diode laser (ECDL) at 1560-nm. The laser output passes through a telecom erbium-doped fiber amplifier (EDFA) and is split in two parts: one part serves as the fundamental wave for SFG; the other part frequency doubled to 780-nm is as another fundamental wave. These two fundamental beams transmit the SFG resonator collinearly to obtain 520-nm laser via a dichromic mirror. In our singly resonant SFG configuration, the fundamental wave at 1560-nm doubly passes the cavity, while the other fundamental wave at 780-nm is maintained resonant with the cavity. The nonlinear medium in the SFG is a quasi-phase-matched PPKTP crystal (both fundamental waves are s-polarized). A Pound Drever-Hall sideband scheme [26] is used to lock the SHG and SFG cavity with the resonant laser frequencies, the modulation frequency of 10.2 and 16 MHz are applied to their own electro-optic modulators (EOM), respectively. The error signal generated from the mixer is fed back to the PZT to maintain the cavity length via an electronic servo loop.

3.1. Three-mirror singly resonant SFG cavity with a variable-reflectivity input coupler

From the perspective of the laser enhanced manner, a three-mirror SFG cavity is equivalent to a two-mirror standing-wave cavity. Different from the two-mirror cavity which takes one concave mirror as the input coupler, it takes an inserted plane mirror instead. The other two concave mirrors (M2 and M3) of the cavity are both highly reflective at 780 and 1560-nm ($R > 99.8\%$) with a curvature radius of $r = 100$ mm, and the plane mirror (M1) is reflective at 780-nm and a high transmissivity at 1560-nm. M3 is output mirror of the cavity, and it has high transmissivity at 520-nm ($T > 97.0\%$). In the experiment, we take the position of M1 as a center of a circle, rotating the set of M1 and M2 simultaneously (see the black dotted bordered rectangle in Figure 1), attaining the continuously tunable reflectivity of the resonator at 780-nm.

The main design idea of the cavity is from Fresnel principle: if the s-polarized light wave reflected at the interface of two media, its reflectivity will be changed with the incident angle:

$$R_s = \frac{[\sin(i_1 - i_2)]^2}{[\sin(i_1 + i_2)]^2} \tag{4}$$

where the i_1 and i_2 represent the incident angle and refractive angle of the s-polarized light. To the three-mirror folded SFG cavity, we tilt the plane input coupler M1 (together with M2); thus, the incident angle between the input coupler M1 and the input 780-nm beam can be varied from 3° to 60°, corresponding to the reflectivity varying from 81.4 to 96.1% (see Figure 3). Such a broad range of the reflectivity is useful for optimizing impedance matching.

For the set of M1 and M2 is rotated integrally with the center of a circle of M1, the equivalent cavity length of the three-mirror cavity between those two concave mirrors is not changed, so the waist radius of resonant laser located in the nonlinear media will not be changed with the tilting. Another advantage of the design is that the resonant lasers are both 0° incident to those two concave mirrors, there does not exit astigmatism in the cavity.

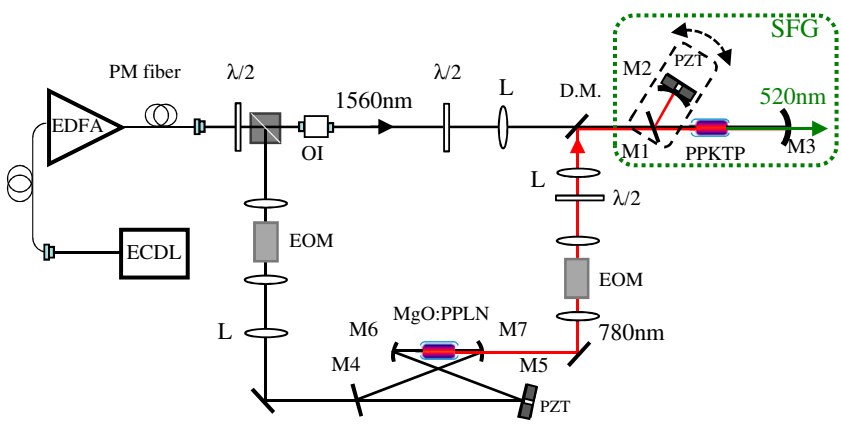

Figure 2. Schematic diagram of the SFG experimental setup. ECDL: external-cavity diode laser; EDFA: erbium-doped fiber amplifier; OI: optical isolator; PM fiber: polarization-maintaining fiber; λ/2: half-wave plate; L: lens; D.M.: dichromatic mirror; PZT: piezoelectric transducer. (The color version of this figure is included in the online version of the journal.)

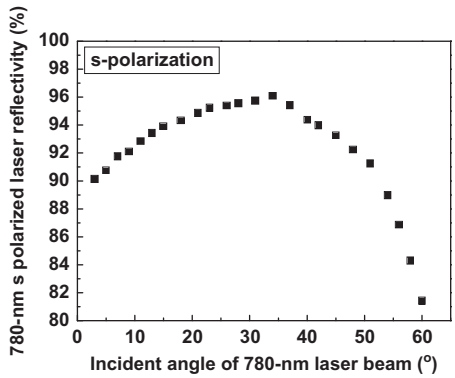

Figure 3. 780-nm s-polarized laser's reflectivity vs. the incident angle of the input coupler M1.

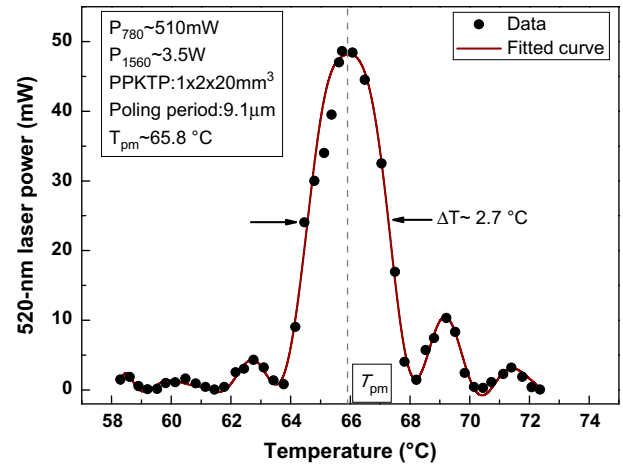

Figure 4. 520-nm laser output power vs. the temperature of PPKTP crystal.

3.2. *Sum-frequency generation to 520-nm laser*

In the experiment, the 780-nm fundamental wave of SFG is obtained by a typical four-mirror bow-tie resonant cavity with a QPM MgO:PPLN crystal (HC Photonics). The dimension of the crystal is 1 mm × 3.4 mm × 25 mm, and the poling period is 19.48 μm. The details of the SHG experiment can be found in Ref. [27]. When the input power at 1560-nm is 2.05 W, a maximum SHG output power of 1.5 W can been achieved.

The generated 780-nm beam combining with 1560-nm beam propagates collinearly through the SFG crystal by a dichromic mirror. Appropriate focusing of the fundamental beams will give higher power intensities in the crystal, and hence a higher nonlinear conversion. The 780-nm laser waist spot radius that we chose is 31 μm, which is determined by the optimum B-K focus factor $\xi = 2.84$ [28]. In order to realize the maximum spatial mode volumes overlap in PPKTP crystal (there is no Poynting vector walk-off in the crystal), the two beams should be the same Rayleigh length [29,30]. The Rayleigh length of 780-nm laser is 14.2 mm to its waist spot radius; thus, the optimum waist spot radius of the 1560-nm laser confirmed finally is 44.2 μm. We take different focus lens to realize the optimum focus to the two fundamental waves, respectively.

The size of the PPKTP crystal (Raicol Crystals Ltd.) used in SFG is 1 mm × 2 mm × 20 mm, with a poling period $\Lambda = 9.1$ μm. The crystal is mounted in a home-made copper oven combined with a thermo-electric cooler. In order to obtain optimum phase-matching temperature in SFG, we measure the temperature tuning curve of the crystal (see the black dots in Figure 4). For a fixed input power at 1560-nm (3.5 W) and 780-nm (510 mW), the optimum phase-matching temperature for the PPKTP crystal is ~65.8 °C, and full width at half maximum is ~2.7 °C. From the experimental results, we can find the temperature tuning curve of the PPKTP crystal is distorted with the standard sin c^2 function, the sub-peaks in right hand side is apparently higher than the left hand side, appearing asymmetric characteristic. And the same characteristic is shown after our repeated measurement at different times. It indicates that the crystal has appeared thermal-induced absorption effect at such power levels. Such thermally induced effect may change the refractive index of the fundamental beams, yields an asymmetric temperature tuning curve. We take "multi-step" theoretical model of refractive index to fit the experimental results, as shown in Figure 4, and a good agreement with the experimental results is obtained [31].

Considering the actual passive loss of the resonator (2% at 1560 nm and 3% at 780-nm, which are fitted by SFG output power with the 780 nm input power at a fixed 1560-nm input power), the nonlinear coupling coefficient (γ_{SFM}) is 1.2%/W, which is measured in a single-pass configuration by just removing the input coupler M1 in the experimental setup and the input powers of the fundamental waves, the optimum reflectivity of the input coupler at 780 nm is ~93% according to the calculation presented in Section 2. So we tilted the input coupler (together with the meniscus mirror M2) to make the 780 nm beam incident angle at 46.3°. We stabilize temperature of the PPKTP crystal at the point of the optimum phase-matched temperature (~65.8 °C). When the input power of 1560 nm is 6.8 W and 1.5 W of 780-nm laser, we get 268 mW of 520-nm laser, which corresponds to a SFG conversion efficiency of ~17.8% for 780-nm laser. Figure 5 shows the experimental results (black squares). The solid line is the theoretical calculation results based on the theoretical analysis in

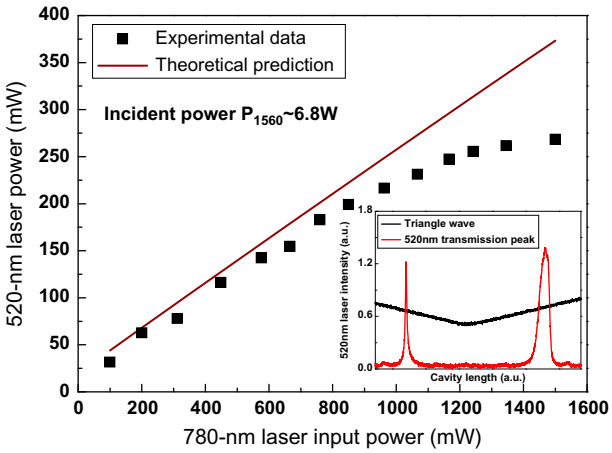

Figure 5. SFG output at 520-nm as a function of 780-nm laser input power. The inset is the asymmetric transmission peak of 520-nm laser monitored by a scanned two-mirror cavity with the SFG crystal. (The color version of this figure is included in the online version of the journal.)

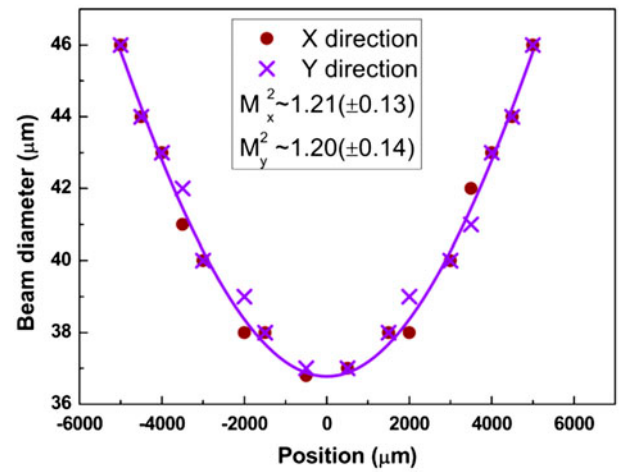

Figure 7. 520-nm laser beam's Gaussian diameters near a focus point along the X and Y directions. The solid lines are fitted curves. (The color version of this figure is included in the online version of the journal.)

Section 2. The experimental results we obtained are basically in agreement with the calculation results; however, the SFG output power is slow deviated when 780-nm laser's incident power exceeds than 800 mW. The main reason may be the thermally induced absorption to the PPKTP crystal.

Similarly, we also measured the 520-nm output power and 780-nm circulating power with the input power at 1560-nm (the 780-nm laser input is 1.6 W). A phase matching temperature of the PPKTP crystal is still controlled at ~65.8 °C. The result is shown in Figure 6. The 780-nm laser circulating power in the SFG cavity is monitored by the 780-nm laser power leaking from M3 when the SFG cavity is locked. The reflectivity of the M3 is known; thus, we can infer the 780-nm circulating power. The output power of 268 mW at 520-nm is lower than the theoretical expected result; we attribute this mainly to the absorption of PPKTP crystal at 520-nm.

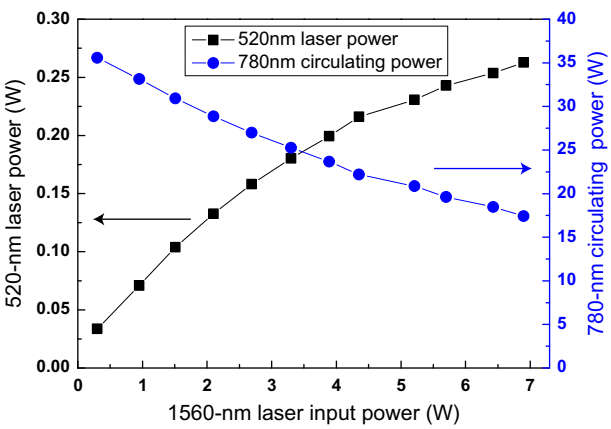

Figure 6. 520-nm output power (squares) and the 780-nm circulating power (dots) vs. the 1560-nm input power. (The color version of this figure is included in the online version of the journal.)

To test this, we take the PPKTP crystal in the SFG experiment placed in a two-mirror standing-wave cavity with a cavity length of 60 mm. The curve radius of two mirrors are both of 30 mm, and they are both high reflective at 520-nm ($R > 97\%$). These components (the two mirrors cavity containing PPKTP crystal) are pumped by another 520-nm s-polarized laser (the same polarized state in our SFG experiment). When the cavity length is scanned by a triangle wave, there appears obvious asymmetric transmission peaks at 520-nm in the rising and falling edges of triangle waves (the inset of Figure 5), such a asymmetric transmission peaks phenomenon shows the characteristic of thermally induced absorption of the SFG crystal to s-polarized 520-nm laser [32,33].

The further improvement to output power is limited by such thermally induced absorption of PPKTP crystal for it absorbed the generated 520-nm laser, and increased the intra-cavity loss of both the fundamental waves gravely. Another method of reduction of the intra-cavity loss can be taken a single-pass configuration of 1560-nm laser instead of the current double-pass configuration.

The knife-blade method is used to measure the 520-nm laser beam quality factor, and the results are shown in Figure 7. The M^2 factors along the X and Y directions are $M_x^2 = 1.21$ (±0.13) and $M_y^2 = 1.20$ (±0.14), respectively.

4. Conclusion

A feasible approach for 520-nm CW green light generation has been presented, using a three-mirror folded singly resonant sum-frequency resonator with an adjustable input coupling by tilting the input coupler mirror. The insensitivity to the input wavelength sets of the sum-frequency cavity makes it suited to the generation of the other visible laser sources. Combined with maturely developed telecom C-band EDFA, when the input power of 1560-nm is 6.8 W and 780-nm laser is 1.5 W, we get 268 mW SFG laser at 520-nm, with a conversion efficiency of 17.8% to the 780-nm laser. The 520-nm CW laser can be used as pump source for a follow-up OPO to generate the practical two-color continuous variable entangled optical fields at 1560 and 780-nm lasers, and this experiment has been done in our laboratory; the experimental results will be published later. Since the 1560-nm laser is the low loss window of the fiber transmission, while the 780-nm laser corresponds to the D_2 line of rubidium, such entangled optical fields are good candidate solution for the quantum repeater. As the pump laser source, 520-nm laser plays an irreplaceable role in the preparation of this entangled optical field.

Funding

This work was supported by the National Major Scientific Research Program of China [grant number 2012CB921601]; the National Natural Science Foundation of China [grants numbers 61475091, 11274213, 61205215, and 61227902], the Shanxi Scholarship Council of China [grant number 2012-015], and the Research Program for Science and Technology Star of Tai Yuan, Shan Xi province, China [grant number 12024707].

References

[1] Robinson, M.P.; Tolra, B.L.; Noel, M.W.; Gallagher, T.F.; Pillet, P. *Phys. Rev. Lett.* **2000,** *85,* 4466–4469.
[2] Gabelica, V.; Rosu, F.; Tabarin, T.; Kinet, C.; Antoine, R.; Broyer, M.; De Pauw, E.D.; Dugourd, P. *J. Am. Chem. Soc.* **2007,** *129,* 4706–4713.
[3] Guo, X.M.; Zhao, J.J.; Li, Y.M. *Appl. Phys. Lett.* **2012,** *100,* 091112.
[4] Guo, X.M.; Xie, C.D.; Li, Y.M. *Phys. Rev. A* **2011,** *84,* 020301(R).
[5] Matsukevich, D.N.; Chanelière, T.; Jenkins, S.D.; Lan, S.Y.; Kennedy, T.A.B.; Kuzmich, A. *Phys. Rev. Lett.* **2006,** *96,* 030405.
[6] Brunner, F.; Innerhofer, E.; Marchese, S.V.; Südmeyer, T.; Paschotta, R. *Opt. Lett.* **2004,** *29,* 1921–1923.
[7] Rothhardt, J.; Eidam, T.; Hädrich, S.; Jansen, F.; Stutzki, F.; Gottschall, T.; Andersen, T.V.; Limpert, J.; Tünnermann, A. *Opt. Lett.* **2011,** *36,* 316–318.
[8] Jensen, O.B.; Andersen, P.E.; Sumpf, B.; Hasler, K.H.; Erbert, G.; Petersen, P.M. *Opt. Express* **2009,** *17,* 6532–6539.
[9] Jensen, O.B.; Petersen, P.M. *Opt. Express* **2013,** *21,* 6076–6081.
[10] Hansen, A.K.; Jensen, O.B.; Andersen, P.E.; Petersen, P.M. *Proc. SPIE* **2014,** *8964,* 896406-1–896406-6.
[11] Pullen, M.G.; Chapman, J.J.; Kielpinski, D. *Appl. Opt.* **2008,** *47,* 1397–1400.
[12] Tu, C.H.; Huang, Z.C.; Lou, K.; Liu, H.J.; Wang, Y.S.; Li, Y.; Lu, F.Y.; Wang, H.T. *Opt. Express* **2010,** *18,* 25183–25191.
[13] Mi, X.Y. *Laser Phys.* **2012,** *22,* 74–77.
[14] Vasilyev, S.; Nevsky, A.; Ernsting, I.; Hansen, M.; Shen, J.; Schiller, S. *Appl. Phys. B* **2011,** *103,* 27–33.
[15] Müller, A.; Jensen, O.B.; Hasler, K.H.; Sumpf, B.; Erbert, G.; Andersen, P.E.; Petersen, P.M. *Opt. Lett.* **2012,** *37,* 3753–3755.
[16] Moutzouris, K.; Sotier, F.; Adler, F.; Leitenstorfer, A. *Opt. Express* **2006,** *14,* 1905–1912.
[17] Dingjan, J.; Darquié, B.; Beugnon, J.; Jones, M.P.A.; Bergamini, S.; Messin, G.; Browaeys, A.; Grangier, P. *Appl. Phys. B* **2006,** *82,* 47–51.
[18] Sané, S.S.; Bennetts, S.; Debs, J.E.; Kuhn, C.C.N.; McDonald, G.D.; Altin, P.A.; Close, J.D.; Robins, N.P. *Opt. Express* **2012,** *20,* 8915–8919.
[19] Mahal, V.; Arie, A. *Opt. Lett.* **1996,** *21,* 1217–1219.
[20] Thompson, R.J.; Tu, M.; Aveline, D.C.; Lundblad, N.; Maleki, L. *Opt. Express* **2003,** *11,* 1709–1713.
[21] Bjarlin Jensen, O.B.; Michael Petersen, P.M. *Appl. Phys. Lett.* **2013,** *103,* 141107.
[22] Mimoun, E.; De Sarlo, L.D.; Zondy, J.J.; Dalibard, J.; Gerbier, F. *Opt. Express* **2008,** *16,* 18684–18691.
[23] Janousek, J.; Johansson, S.; Tidemand-Lichtenberg, P.T.; Wang, S.H.; Mortensen, J.L.; Buchhave, P.; Laurell, F. *Opt. Express* **2005,** *13,* 1188–1192.
[24] Schori, C.; Sørensen, J.L.; Polzik, E.S. *Phys. Rev. A* **2002,** *66,* 033802.
[25] Vance, J.D.; She, C.Y.; Moosmüller, H. *Appl. Opt.* **1998,** *37,* 4891–4896.
[26] Drever, R.W.P.; Hall, J.L.; Kowalski, F.V.; Hough, J.; Ford, G.M.; Munley, A.J.; Ward, H. *Appl. Phys. B* **1983,** *31,* 97–105.
[27] Ge, Y.L.; Guo, S.L.; Han, Y.S.; Wang, J.M. *Opt. Commun.* **2015,** *334,* 74–78.
[28] Boyd, G.D.; Kleinman, D.A. *J. Appl. Phys.* **1968,** *39,* 3597–3639.
[29] Mimoun, E.; De Sarlo, L.D.; Zondy, J.J.; Dalibard, J.; Gerbier, F. *Appl. Phys. B* **2010,** *99,* 31–40.
[30] Guha, S.; Falk, J. *J. Appl. Phys.* **1980,** *51,* 50–60.
[31] Guo, S.L.; Ge, Y.L.; Han, Y.S.; He, J.; Wang, J.M. *Opt. Commun.* **2014,** *326,* 114–120.
[32] Han, Y.S.; Wen, X.; Bai, J.D.; Yang, B.D.; Wang, Y.H.; He, J.; Wang, J.M. *J. Opt. Soc. Am. B* **2014,** *31,* 1942–1947.
[33] Zhai, Y.Y.; Fan, B.; Yang, S.F.; Zhang, Y.; Qi, X.H.; Zhou, X.J.; Chen, X.Z. *Chin. Phys. Lett.* **2013,** *30,* 044209.

Appendix 1

Singly resonant SFG can be characterized by the passive loss δ, the input laser frequency ω, the reflectance of the input coupler R_i, and the nonlinear coupling coefficient γ_{SFM}. According to the small-signal approximation, the SFG output power can be expressed as

$$P_3 = \gamma_{SFM} P_{c,1} P_{c,2}, \tag{A1}$$

where γ_{SFM} shows the single-pass SFG conversion efficiency of the crystal for the two fundamental waves, and $P_{c,1}$ ($i = 1, 2$) represents the circulating optical powers in the resonator at 1560 and 780-nm lasers.

The nonlinear conversion depletion δ_1^{NL}, δ_2^{NL} for two fundamental waves can be written as

$$\delta_1^{NL} = \frac{\omega_1}{\omega_1 + \omega_2}\gamma_{SFM}P_{c,2}, \tag{A2}$$

$$\delta_2^{NL} = \frac{\omega_2}{\omega_1 + \omega_2}\gamma_{SFM}P_{c,1}, \tag{A3}$$

The first terms in Equations (A2) and (A3) are the ratios of frequencies of the two fundamental waves (ω_1 is at 1560-nm and ω_2 is at 780-nm). Nonlinear conversion depletion for one fundamental beam in SFG is not a constant but a variable of the power circulating of the other fundamental wave, and they are affected by each other.

The percent of residual power in the resonator after one round trip for 1560 and 780-nm is

$$R_{m,1} = 1 - (\delta_1 + \delta_1^{NL}), \tag{A4}$$

$$R_{m,2} = 1 - (\delta_2 + \delta_2^{NL}), \tag{A5}$$

The enhancement factor describes the resonator enhancement of the fundamental wave and is defined as the ratio between the optical power circulating in the resonator and the power incident on the resonator. When the fundamental wave is in resonance, the enhancement factor can be reduced to the Fabry–Perot model. Considering the nonlinear conversion depletion and the passive loss of the resonator, the enhancement factor of the two fundamental waves can be written as

$$E_1 = \frac{P_{c,1}}{P_{i,1}} = \frac{1 - R_{i,1}}{[1 - \sqrt{R_{i,1}R_{m,1}}]^2}, \tag{A6}$$

$$E_2 = \frac{P_{c,2}}{P_{i,2}} = \frac{1 - R_{i,2}}{[1 - \sqrt{R_{i,2}R_{m,2}}]^2}, \tag{A7}$$

where $P_{i,1}$ ($P_{i,2}$) represents the power at 1560 nm (780 nm) incident on the resonator, and $R_{i,1}$ ($R_{i,2}$) represents reflectivity of the input coupler at 1560 nm (780 nm). Note that $P_{c,1}$ is a function of $R_{m,2}$ and $R_{i,1,}$ and the same way to the $P_{c,2}$.

In our experiment, the 1560 nm beam is not in resonance with the resonator (double-pass through the crystal), so its percent residual intra-cavity power after one round trip simplifies to

$$P_{c,1} = P_{i,1}[1 - (\delta_1 + \delta_1^{NL})]. \tag{A8}$$

Substituting Equations (A2)–(A5) into Equations (A7) and (A8) yields a set of simultaneous equations for the intra-cavity power at 1560 and 780 nm:

$$P_{c,1} = P_{i,1}\left[1 - \left(\delta_1 + \frac{\omega_1}{\omega_1 + \omega_2}\gamma_{SFM}P_{c,2}\right)\right], \tag{A9}$$

$$P_{c,2} = P_{i,2}\frac{1 - R_{i,2}}{\left\{1 - \left\{R_{i,2}\left[1 - \left(\delta_2 + \frac{\omega_2}{\omega_1+\omega_2}\gamma_{SFM}P_{c,1}\right)\right]\right\}^{1/2}\right\}^2}. \tag{A10}$$

By solution of the simultaneous equation, the singly resonant SFG output power can be characterized from Equation (A1).